Advances in Nanoparticles, 2015, 4, 45-52
Published Online May 2015 in SciRes. http://www.scirp.org/journal/anp
http://dx.doi.org/10.4236/anp.2015.42006

Structural and Optical Properties of $Mg_{1-x}Zn_xFe_2O_4$ Nano-Ferrites Synthesized Using Co-Precipitation Method

Abdalrawf I. Ahmed[1], Mohamed A. Siddig[1*], Abdulmajid A. Mirghni[1,2], Mohamed I. Omer[3], Abdelrahman A. Elbadawi[1]

[1]Department of Physics, Faculty of Science and Technology, Alneelain University, Khartoum, Sudan
[2]Department of Physics, Faculty of Education, Al Fashir University, Al Fashir, Sudan
[3]Department of Physics, Faculty of Science and Technology, Nile Valley University, Atbara, Sudan
Email: *siddig_ma@yahoo.com

Received 31 March 2015; accepted 5 May 2015; published 8 May 2015

Abstract

In this work, the $Mg_{1-x}Zn_xFe_2O_4$ Nanoferrites (where x = 0.0, 0.2, 0.4, 0.6 and 0.8) was synthesized using co-precipitation method. The investigation of structural and optical properties was carried out for the synthesized samples using X-ray diffraction (XRD), Fourier transform infrared spectroscopy (FTIR) and Ultraviolet visible spectrophotometer (UV-Vis). XRD revealed that the structure of these nanoparticles is spinel with space group Fd3m and crystallite size lies in the range 21.0 - 42.8 nm. Lattice parameter was found to increases with Zn concentration and this may be due to the larger ionic radius of the Zn^{2+} ion. FTIR spectroscopy confirmed the formation of spinel ferrite and showed the characteristics absorption bands around 612, 1146, 1404, 1649 and 3245 cm^{-1}. The energy band gap was calculated for samples with different ratio and was found to be 4.77, 4.82, 4.86, 4.87 and 4.95 eV. The substitution was resulted in slight increased in the lattice constant and that sequentially may lead to the slightly decreased in the energy gap.

Keywords

Co-precipitation Method, Ferrite Nanoparticles, Spinel Structure, XRD

1. Introduction

Nanotechnology is one of the leading scientific fields today since it combines knowledge from the fields of Physics, Chemistry, Biology, Medicine and Engineering. The application and use of nanomaterials are extensive

*Corresponding author.

How to cite this paper: Ahmed, A.I., Siddig, M.A., Mirghni, A.A., Omer, M.I. and Elbadawi, A.A. (2015) Structural and Optical Properties of $Mg_{1-x}Zn_xFe_2O_4$ Nano-Ferrites Synthesized Using Co-Precipitation Method. *Advances in Nanoparticles*, **4**, 45-52.
http://dx.doi.org/10.4236/anp.2015.42006

such as in electronic and mechanical devices, optical magnetic components, tissue engineering magnetic storage systems and magnetic resonance imaging [1] [2]. Nanotechnology and material technology are new techniques for synthesis and processing manipulation and assembly using natures own building blocks (atoms, molecules or macromolecules) for the intelligent design of functional materials, components and systems with attractive qualities and functions [3] [4].

Ferrites are well-known magnetic nanomaterials intensively studied as a recording media due to their superior physical properties. These properties make ferrites an ideal candidate for technical applications such as magnetic resonance imaging enhancement, catalysis, sensors and pigments [5]. Mixed spinel ferrites have been studied intensively over the last few years due to their potential applications. Spinel ferrites have the chemical formula MFe_2O_4 in which M can be any divalent metal cations. In spinel ferrite, oxygen forms face centre cubic (FCC) lattice with divalent cations at tetrahedral (A) and/or octahedral (B) sites. Magnesium ferrite ($MgFe_2O_4$) has an inverse spinel structure with the preference of Mg^{2+} cations mainly on octahedral sites [6]-[9], while Zinc ferrite ($ZnFe_2O_4$) has normal spinel structure, in which Zn^{2+} cations mainly occupy tetrahedral sites [6] [10].

The small scale size of the well-known spinel ferrites has opened up the door for intensive research to utilize their properties for biomedical applications [11]-[13]. Numerous methods were reported in literature showing the possibilities of producing particle with size in the range of 2 - 100 nm. Among these methods are co-precipitation, hydrothermal and sol-gel Methods [14] [15], which were reported to be fast and producing high quality nanoparticles.

In this work, $Mg_{1-x}Zn_xFe_2O_4$ nanoferrites where x = 0.0, 0.2, 0.4, 0.6 and 0.8) were synthesized using co-precipitation methods. X-ray diffraction (XRD) was used in order to investigate the structural of Zn substituted magnesium nano-ferrites and to determine the lattice parameters and the space group symmetry. Ultraviolet visible spectrometer (UV vis) and Fourier Transform Infrared Spectroscopy (FTIR) were used to investigate the optical properties of crystallite nanoparticles.

2. Material and Method

Mg Zn ferrite ($Mg_{1-x}Zn_xFe_2O_4$) nanoparticles with composition (x = 0.0, 0.2, 0.4, 0.6 and 0.8) was prepared by the co-precipitation method. **Figure 1** shows the synthesis scheme for nanoparticles production. Stoichiometric amounts from pure raw materials of $Fe(NO_3)_3{\cdot}9H_2O$, $Mg(NO_3)_2{\cdot}6H_2O$, $Zn(NO_3)_2{\cdot}6H_2O$, and NaOH were used to prepare the required solutions with required molarities. The solution of $Fe(NO_3)_3{\cdot}9H_2O$, 0.4 M (25 ml), $Mg(NO_3)_2{\cdot}6H_2O$ 0.2M (25 ml) and $Zn(NO_3)_2{\cdot}6H_2O$ were first mixed and then slowly added 3Molarity of NaOH (25 ml) solution under stirring of 3000 rpm for 30 minutes to obtain a mixture of pH 11 - 13. The colloidal solution was then kept in a water bath at 80˚C for 1 hour to assure removal of $NaNO_3$ from the powder. The produced precipitate was washed 10 times with hot deionized water until the filtrate had a pH 7 [16] [17]. Then the

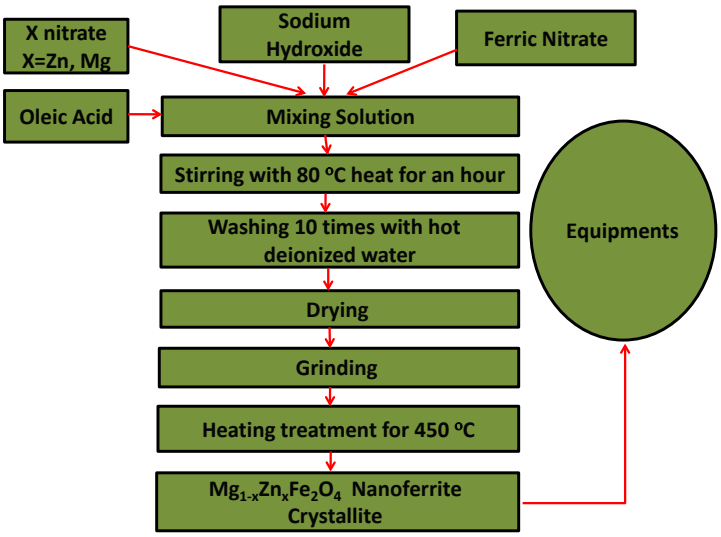

Figure 1. Synthesis scheme for nanoparticles production.

samples were dried and grinned to absolute powder and annealed to 450˚C for 6 hours in temperature controlled muffle furnace Vulcan A-550 at a heating rate 10˚C/min.

The XRD analysis was carried out to confirm the purity of the synthesize materials using Shimadzu 6000 X-ray diffractometer with Cu-kα radiation of a wavelength λ = 1.5406 Å source.

FTIR measurements were performed using (Mattson, model 960m0016) spectra, while the absorption of solution with different concentration was calculated using UV min 1240 spectrometer Shimadzy.

3. Results and Discussion

3.1. Crystal Analysis

Determination of the crystal structure, the lattice parameters and the space group symmetry are importance in the study of structural, electrical and optical properties of the nanoparticle ferrites. The information of single phase $Mg_{1-x}Zn_xFe_2O_4$ is confirmed after analyzing the x-ray diffraction pattern by MDI Jade 5.0, ORIGAN and FULLPROF. The crystal structure is found to be cubic with space group Fd3m. The X-ray diffraction (XRD) is carried out at room temperature. **Figure 2** shows the X-ray diffraction patterns for the sample $MgFe_2O_4$ nanoparticles with x = 0.0, while **Figure 3** shows the X-ray diffraction patterns for the samples $Mg_{1-x}Zn_xFe_2O_4$ nanoparticles with different composition (x = 0.2, 0.4, 0.6 and 0.8). The peaks were indexed as (111), (220), (311), (222), (400), (422), (511), (440), and (533). The crystallite size, lattice constants, volume and densities are listed in **Table 1**. The crystal size is calculated using the Debye-Scherer's equation [18]:

$$D = \frac{0.9\lambda}{\beta \cos\theta} \tag{1}$$

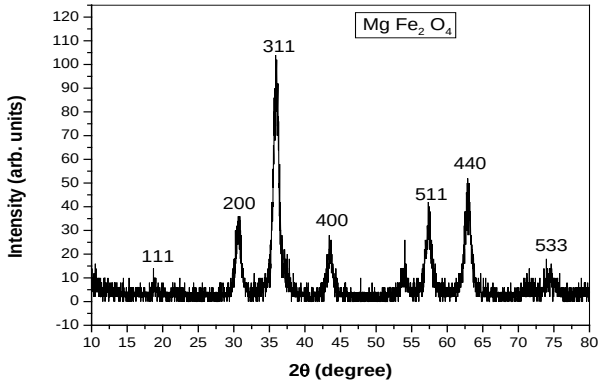

Figure 2. XRD patterns of $Mg_{1-x}Zn_xFe_2O_4$ nano-ferrites for x = 0.

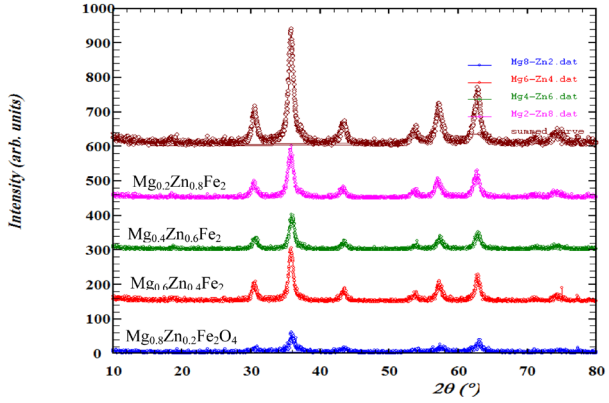

Figure 3. XRD patterns of $Mg_{1-x}Zn_xFe_2O_4$ nano-ferrites for x = 0.2, 0.4, 0.6 and 0.8.

Table 1. Particle size (D), Lattice constant (a), Volume and Density of $Mg_{1-x}Zn_xFe_2O_4$ nano-ferrites.

No.	Samples	Crystal size (nm)	Lattice constant (Å)	Volume (nm^{-3})	Density (g/cm^3)
1	$MgFe_2O_4$	42.8	8.09	529.5	5.175
2	$Mg_{0.8}Zn_{0.2}Fe_2O_4$	26.6	8.38	587.4	4.522
3	$Mg_{0.6}Zn_{0.4}Fe_2O_4$	24.1	8.39	590.0	4.502
4	$Mg_{0.4}Zn_{0.6}Fe_2O_4$	21.0	8.40	591.9	5.176
5	$Mg_{0.2}Zn_{0.8}Fe_2O_4$	23.2	8.44	601.5	5.070

where D is the average crystallite size, θ is the diffraction angle, λ is the wavelength of incident X-ray and β is the full width at half maximum (FWHM) of the (XRD) peak in units of radians. The crystallite size vs. Zn concentration is plotted in **Figure 4** and the crystallite size is found to scattered in the range 21 - 42.8 nm for different compositions. In the obtained diffraction pattern the lattice constants are found to increase from (8.09 - 8.44 Å) as the Zn concentration increased. The particle size of the nanocrystalline samples, calculated from the XRD data using Equation (1), are remained within the range (21.0 - 42.8 nm). The increased in lattice constant with Zn concentration may be due to the fact that Zn^{2+} ions (0.82 Å) is larger than that of the Mg^{2+} ions (0.72 Å). Addition of Zn^{2+} at the expense of Mg^{2+} in the ferrite is expected to increase the lattice constant. The lattice parameter (a) is estimated using lattice spacing (d) values and respective miller indices (hkl). The lattice constant (a) was calculated by MDI Jade 5.0 program and using the equation [19]:

$$a = \frac{d}{\left(h^2 + k^2 + l^2\right)^{1/2}} \tag{2}$$

where a is the lattice parameter, d is the lattice spacing and h, k, l are the miller indices. The lattice parameter is obtained using XRD data lies in the range of 8.1 - 8.4 Å for different Zn concentration as shown in **Figure 5**. It increases with increasing Zn concentration due to the larger ionic radius of Zn^{2+} (0.08 nm) Cation as compared to ionic radius of Mg^{2+} (0.06 nm) Cation [20] [21].

3.2. FTIR Analysis

In order to investigate the chemical functional groups on the the synthesized $Mg_{1-x}Zn_xFe_2O_4$, FTIR spectroscopy are performed. The FTIR of nanocrystals powders (as pellets in KBr) in the range of 400 cm^{-1} to 4000 cm^{-1} is shown in **Figure 6** for pure sample where x = 0. The FTIR of $Mg_{1-x}Zn_xFe_2O_4$ nano-ferrites powders for samples where x = 0.2, 0.4, 0.6 and 0.8 is plotted and shown in **Figure 7**. The bands (υ_1, υ_2) for the samples are found to be in range 3148 - 3450 cm^{-1} and 1644 - 1649 cm^{-1}, respectively. These observed bands maybe are due to the O-H stretching vibration of the free absorbed water and indicates the existence of hydroxyl groups in the synthesized ferrites, which is observed in previous experiments [22] [23]. The band (υ_3) for the samples are observed around 1404 cm^{-1} and is attributed to the C=O stretching vibration of the carboxyl group. In range 1107 - 1147 cm^{-1}, the band (υ_4) is observed and is related to the stretching vibration due to nitrate group [24] [25]. In the range of 800 - 400 cm^{-1}, two main absorption bands with very low intensity are observed around 400 and 600 cm^{-1} and may be is caused by metal oxygen vibration in the octahedral side. The υ_1, υ_2, υ_3, υ_4 and υ_5 are absorption bands around 3148 - 3450, 1644 - 1649, 1404, 1107 - 1147 and 612 - 663 cm^{-1}, respectively for the samples with different compositions and are attributed to the vibration of the tetrahedral and octahedral metal-oxygen (M-O) bands in the lattices of the synthesized nanocrystals. The FTIR frequency bands for various Zn and Mg contents are listed in **Table 2**.

3.3. UV Visible Analysis

The absorption as a function of wavelength for sample $Mg_{0.6}Zn_{0.4}Fe_2O_4$ is shown in **Figure 8**. Maximum absorption for the sample is observed at wavelength 232.4 nm. Several models are used to determine the optical properties of nano ferrites. The most widespread is the Tauc model which allows the derive of the band gap energy E_g from $(\alpha h\upsilon)^2$ as function of the incident energy ($h\upsilon$). The Tauc optical gap associated with the $Mg_{1-x}Zn_xFe_2O_4$ nano ferrites is determine through an extrapolation of the linear trend observed in the spectral

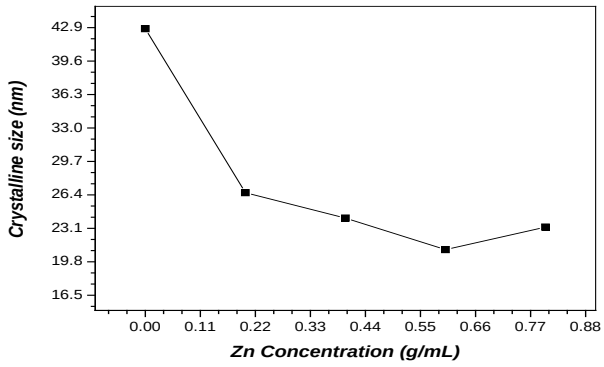

Figure 4. Particle size as a function of Zn concentration of $Mg_{1-x}Zn_xFe_2O_4$ nano-ferrites.

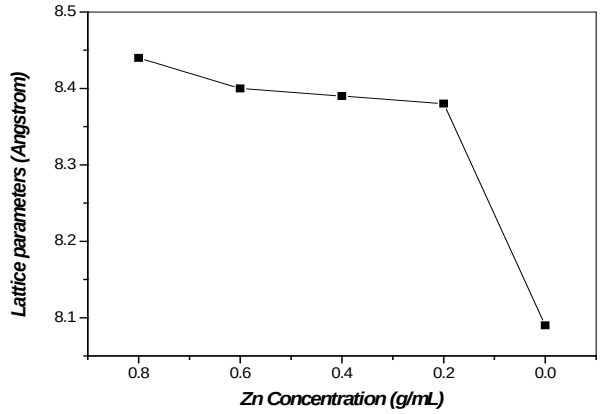

Figure 5. Lattice parameter as a function of Zn concentration of $Mg_{1-x}Zn_xFe_2O_4$ nano-ferrites.

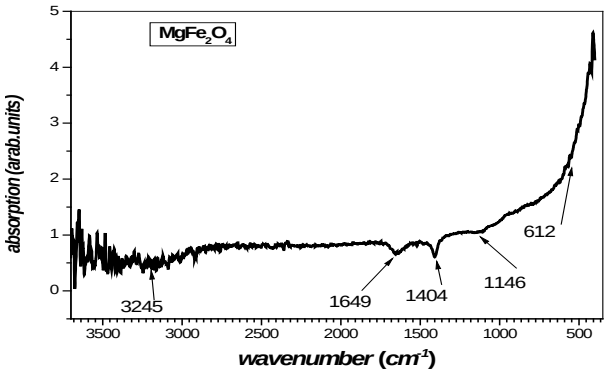

Figure 6. The FTIR spectrum of $Mg_{1-x}Zn_xFe_2O_4$ nano-ferrites for x = 0.

dependence of $(\alpha h\upsilon)^2$ over a limited range of photon energies $h\upsilon$. The Tauc optical gap is defined as occurring at the intercept of this linear extrapolation with Y axis. The absorption coefficient α near the band edge in many Nano ferrites shows an exponential upon photon energy usually obeying the relation [26]:

$$(\alpha h\upsilon) = A\left(h\upsilon - E_g\right)^n \tag{3}$$

where, α is the absorption coefficient and A is known as edge width parameter, E_g is the energy band gap, n = (1/2, 1, 2) is the a constant dependent on the degree of transition, ($h\upsilon$) is incident photon energy. The band gap is

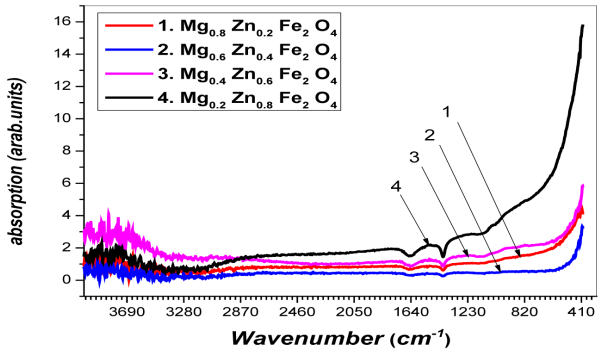

Figure 7. The FTIR spectrum of $Mg_{1-x}Zn_xFe_2O_4$ nano-ferrites for x = 0.2, 0.4, 0.6 and 0.8.

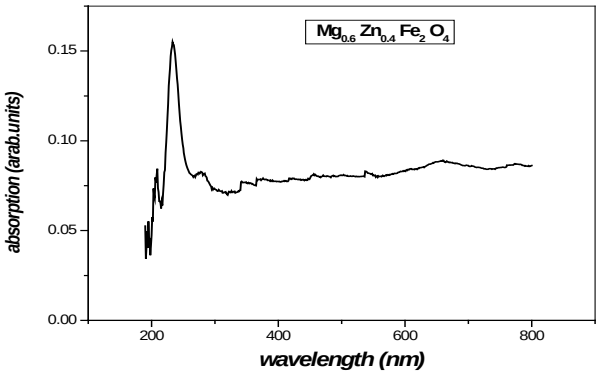

Figure 8. Absorption as a function of wavelength for sample of $Mg_{0.6}Zn_{0.4}Fe_2O_4$ composition.

Table 2. Wave numbers, wavelength, and energy band gaps of $Mg_{1-x}Zn_xFe_2O_4$ nano-ferrites.

No.	Samples	υ_1	υ_2	υ_3	υ_4	υ_5	Energy gap E_g (eV)
1	$MgFe_2O_4$	3245	1649	1404	1146	612	4.77
2	$Mg_{0.8}Zn_{0.2}Fe_2O_4$	3245	1649	1404	1146	612	4.82
3	$Mg_{0.6}Zn_{0.4}Fe_2O_4$	3450	1649	1404	1107	663	4.86
4	$Mg_{0.4}Zn_{0.6}Fe_2O_4$	3148	1644	1404	1140	612	4.87
5	$Mg_{0.2}Zn_{0.8}Fe_2O_4$	3419	1649	1404	1120	613	4.95

then evaluated by plotting ($h\upsilon$) versus $(\alpha h\upsilon)^2$ and extrapolating the tangent on the X-axis (Tauc plots). **Figure 9** shows Tauc plot method for sample of $MgFe_2O_4$, and the energy band gap are found to be 4.77, 4.82, 4.86, 4.87 and 4.95 eV for samples with different concentration (x = 0.2, 0.4, 0.6 and 0.8), respectively.

4. Conclusion

$Mg_{1-x}Zn_xFe_2O_4$ nanparticles was prepared successfully using co-precipitation method. The formation of single phase crystallite structure with size in the range 21.0 - 42.8 nm was confirmed by X-ray diffraction. Lattice parameter was found to increase with Zn concentration and this may be due to the larger ionic radius of the Zn^{2+} ion. FTIR spectrum exhibited expected main absorption bands, thereby confirming the spinel structure. Optical band gap energy $Mg_{1-x}Zn_xFe_2O_4$ nanoferrite was found to be in the range 4.77 to 4.95 eV for samples with different ratio of Mg Zn. The synthesized nanoferrites are expected to be useful in several technological applications such as soft magnets and magnetic fluids for hyperthermia. The structural and properties of spinel ferrites

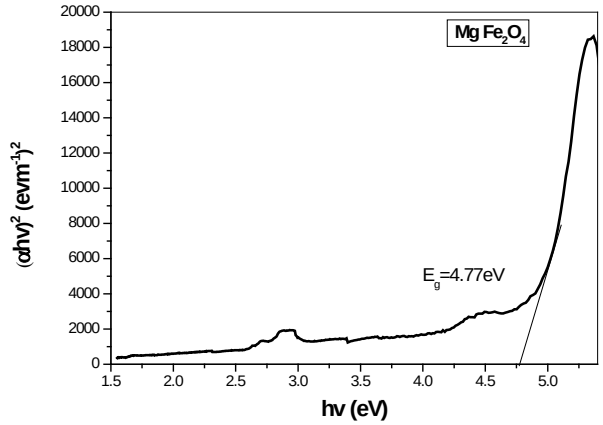

Figure 9. Plot of $(\alpha h\nu)^2$ versus $h\nu$ for $MgFe_2O_4$ nano-ferrites.

depend upon the method of preparation, the nature of substitutional element and the concentration of the substitution element. Attempts can be made to prepare the samples by different methods to get desired properties and crystallite size.

Acknowledgements

Abdalrawf I. Ahmed would like to thank the department of physics particularly material laboratory, Al-neelain University, Sudan for supporting this research.

References

[1] Flores-Acosta, M., Sotelo-Lerma, M., Arizpe-Chavez, H., Castillon-Barraza, F.F. and Ramirez-Bon, R.J. (2003) Excitonic Absorption of Spherical PbS Nanoparticles in Zeolite A. *Solid State Communications*, **128**, 407-411. http://dx.doi.org/10.1016/j.ssc.2003.09.008

[2] Pulisova, P., Kovac, J., Voigtd, A. and Raschman, P. (2013) Structure and Magnetic Properties of Co and Ni Nano-Ferrites Prepared by a Two Step Direct Microemulsions Synthesis. *Journal of Magnetism and Magnetic Materials*, **341**, 93-99. http://dx.doi.org/10.1016/j.jmmm.2013.04.003

[3] Lodhi, M.Y., Mahmood, K., Mahmood, A., Malika, H., Warsi, M.F., Shakir, I., Asghar, M. and Khan, M.A. (2014) New $Mg_{0.5}Co_xZn_{0.5-x}Fe_2O_4$ Nano-Ferrites: Structural Elucidation and Electromagnetic Behavior Evaluation. *Current Applied Physics*, **14**, 716-720. http://dx.doi.org/10.1016/j.cap.2014.02.021

[4] Jan, L.S., Radiman, S., Siddig, M.A., Muniandy, S.V., Hamid, M.A. and Jamali, H.D. (2004) Preparation of Nanoparticles of Polystyrene and Polyaniline by γ-Irradiation in Lyotropic Liquid Crystal. *Colloids and Surfaces A*: *Physicochemical and Engineering Aspects*, **251**, 43-52. http://dx.doi.org/10.1016/j.colsurfa.2004.09.025

[5] Mathew, D.S. and Juaug, R.-S. (2007) An Overview of the Structure and Magnetism of Spinel Ferrite Nanoparticles and Their Synthesis in Micro Emulsions. *Chemical Engineering Journal*, **129**, 51-65. http://dx.doi.org/10.1016/j.cej.2006.11.001

[6] Rahman, S., Nadeem, K., Anis-ur-Rehman, M., Mumtaz, M., Naeem, S. and Letofsky-Papst, I. (2013) Structural and Magnetic Properties of ZnMg-Ferrite Nanoparticles Prepared Using the Co-Precipitation Method. *Ceramics International*, **39**, 5235-5239. http://dx.doi.org/10.1016/j.ceramint.2012.12.023

[7] Pradeep, A., Priyadharsini, P. and Chandrasekaran, G. (2008) Sol-Gel Route of Synthesis of Nanoparticles of $MgFe_2O_4$ and XRD, FTIR and VSM Study. *Journal of Magnetism and Magnetic Materials*, **320**, 2774-2779. http://dx.doi.org/10.1016/j.jmmm.2008.06.012

[8] Greenwood, N.N. and Earnshaw, A. (1984**)** Chemistry of the Elements; Pergamon Press Ltd., Oxford, 279.

[9] Ichiyanagi, Y., Kubota, M., Moritake, S., Kanazawa, Y., Yamada, T. and Uehashi, T. (2007) Magnetic Properties of Mg-Ferrite Nanoparticles. *Journal of Magnetism and Magnetic Materials*, **310**, 2378-2380. http://dx.doi.org/10.1016/j.jmmm.2006.10.737

[10] Thummer, K.P., Chhantbar, M.C., Modi, K.B., Baldha, G.J. and Joshi, H.H. (2004) Localized Canted Spin Behaviour in $Zn_xMg_{1.5-x}Mn_{0.5}FeO_4$ Spinel Ferrite System. *Journal of Magnetism and Magnetic Materials*, **280**, 23-30. http://dx.doi.org/10.1016/j.jmmm.2004.02.017

[11] Kumara, C.S.S.R. and Mohammad, F. (2011) Magnetic Nanomaterials for Hyperthermia-Based Therapy and Controlled Drug Delivery. *Advanced Drug Delivery Reviews*, **63**, 789-808. http://dx.doi.org/10.1016/j.addr.2011.03.008

[12] Giri, J., Pradhan, P., Somani, V., Chelawat, H., Chhatre, S., Banerjee, R. and Bahadur, D. (2008) Synthesis and Characterizations of Water-Based Ferrofluids of Substituted Ferrites [$Fe_{1-x}B_xFe=O_4$, B=Mn, Co (x=0−1)] for Biomedical Applications. *Journal of Magnetism and Magnetic Materials*, **320**, 724-730. http://dx.doi.org/10.1016/j.jmmm.2007.08.010

[13] Sharifi, I., Shokrollahi, H. and Amiri, S. (2012) Ferrite-Based Magnetic Nanofluids Used in Hyperthermia Applications. *Journal of Magnetism and Magnetic Materials*, **324**, 903-915. http://dx.doi.org/10.1016/j.jmmm.2011.10.017

[14] Chen, Y., Ruan, M., Jiang, Y.F., Cheng, S.G. and Li, W. (2010) The Synthesis and Thermal Effect of $CoFe_2O_4$ Nanoparticles. *Journal of Alloys and Compounds*, **493**, L36-L38. http://dx.doi.org/10.1016/j.jallcom.2009.12.170

[15] Liu, Q., Sun, J.H., Long, H.R., Sun, X.Q., Zhong, X.J. and Xu, Z. (2008) Hydrothermal Synthesis of $CoFe_2O_4$ Nanoplatelets and Nanoparticles. *Materials Chemistry and Physics*, **108**, 269-273. http://dx.doi.org/10.1016/j.matchemphys.2007.09.035

[16] Omer, M.I.M., Elbadawi, A.A. and Yassin, O.A. (2013) Synthesis and Structural Properties of $MgFe_2O_4$ Ferrite Nano-Particle. *Journal of Applied and Industrial Sciences*, **1**, 20-23.

[17] Ali, R., Khan, M.A., Mahmood, A., Chughtai, A.H., Sultan, A., Shahide, M., Ishaq, M. and Wars, M.F. (2014) Structural, Magnetic and Dielectric Behavior of $Mg_{1-x}Ca_xNi_yFe_{2-y}O_4$ Nano-Ferrites Synthesized by the Micro-Emulsion Method. *Ceramics International*, **40**, 3841-3846. http://dx.doi.org/10.1016/j.ceramint.2013.08.024

[18] Ahmed, M.A., Rady, K.E.S., El-Shokrofy, K.M., Arais, A.A. and Shams, M.S. (2014) The Influence of Zn^{2+} Ions Substitution on the Microstructure and Transport Properties of Mn-Zn Nanoferrites. *Materials Sciences and Applications*, **5**, 932-942. http://dx.doi.org/10.4236/msa.2014.513095

[19] Mittal, V.K., Chandramohan, P., Santanu, B., Srinivasan, M.P., Velmurugan, S. and Narasimhan, S.V. (2006) Cation Distribution in $Ni_xMg_{1-x}Fe_2O_4$ Studied by XPS and Mössbauer Spectroscopy. *Solid State Communications*, **137**, 6-10. http://dx.doi.org/10.1016/j.ssc.2005.10.019

[20] Ladgaonkar, B.P., Vasambekar, P.N. and Vaingankar, A.S. (2000) Cation Distribution and Magnetisation Study of Nd^{+3} Substituted Zn-Mg Ferrites. *Journal of Magnetism and Magnetic Materials*, **210**, 289-294. http://dx.doi.org/10.1016/S0304-8853(99)00468-0

[21] Maensiri, S., Masingboon, C., Boonchom, B. and Seraphin, S. (2007) A Simple Route to Synthesize Nikel Ferrite ($NiFe_2O_4$) Nanoparticles Using Egg White. *Scripta Materialia*, **56**, 797-800. http://dx.doi.org/10.1016/j.scriptamat.2006.09.033

[22] Dey, S., Roy, A., Das, D. and Ghose, J. (2004) Preparation and Characterization of Nanocrystalline Disordered Lithium Ferrite by Citrate Precursor Method. *Journal of Magnetism and Magnetic Materials*, **270**, 224-229. http://dx.doi.org/10.1016/j.jmmm.2003.08.024

[23] Priyadharsini, P., Pradeep, A., Sambasiva, P. and Chandrasekaran, G. (2009) Structural, Spectroscopic and Magnetic Study of Nanocrystalline Ni-Zn Ferrites. *Materials Chemistry and Physics*, **116**, 207-213. http://dx.doi.org/10.1016/j.matchemphys.2009.03.011

[24] Hankare, P.P., Patil, R.P., Jadhav, A.V., Pandav, R.S., Garadkar, K.M., Sasikala, R. and Tripathi, A.K. (2011) Synthesis and Characterization of Nanocrystalline Ti-Substituted Zn Ferrite. *Journal of Alloys and Compounds*, **509**, 2160-2163. http://dx.doi.org/10.1016/j.jallcom.2010.10.173

[25] Sánchez-Vergara, M.E., Alonso-Huitron, J.C., Rodriguez-Gómez, A. and Reider-Burstin, J.N. (2012) Determination of the Optical GAP in Thin Films of Amorphous Dilithium Phthalocyanine Using the Tauc and Cody Models. *Molecules*, **17**, 10000-10013. http://dx.doi.org/10.3390/molecules170910000

[26] Jan, L.S. and Siddig, M.A. (2011) Synthesis, Characterization and Enhanced Electrical Properties of CTAB-Directed Polyaniline Nanoparticles. *Chinese Journal of Polymer Science*, **29**, 181-190. http://dx.doi.org/10.1007/s10118-010-1016-4